CMR Imaging of Profound Macrovascular Obstruction

Anurag Sahu, M.D., FACC[1]; Gary McNeal, BS[2]

[1]*Emory University Hospital, Atlanta, GA, USA*
[2]*Siemens Healthcare, MR RD Cardiac Collaboration, Hoffman Estates, IL, USA*

Introduction

Cardiac cine imaging of the myocardium may be used to assess wall motion abnormalities, wall thinning, the presence of tumor and thrombus, and morphological variants in a wide variety of cardiac syndromes and conditions. Dynamic first-pass myocardial perfusion imaging may be used to assess the myocardium for reversible ischemia, irreversible ischemia, microvascular and macrovascular obstruction. Delayed myocardial enhancement imaging may be used to assess myocardial viability in the setting of chronic and acute infarct, as well as a host of other non-ischemic cardiomyopathies. In this case report, all three techniques were used to collectively assess for myocardial viability in a patient presenting with chest pain.

Patient history

42-year-old male with a history of diabetes mellitus presented to an outside hospital with complaints of chest pain. He was found to have ST elevation in the anterior leads and received thrombolytic therapy. His ST segment elevation did not resolve and chest pain resolution did not occur for a period of 24 hours. Four days later he was transferred to our institution for consideration of bypass surgery versus interventional therapy for obstructive coronary artery disease. Echocardiography illustrated severely depressed LV function with akinetic anterior wall. Cardiac MRI was requested for assessment of LV function, myocardial viability, and to evaluate for possible left ventricular thrombus.

Methods

All imaging was performed on a 1.5T Siemens MAGNETOM Avanto, software version *syngo* MR B17, using a 6-channel anterior body array coil and the 6-channel spine array coil. Initial pre-contrast cardiac cine imaging of the myocardium was performed in short axis and long axis views with a segmented TrueFISP pulse sequence (Fig. 1): TR 38.8 ms, TE 1.2 ms, flip angle (FA) 66°, field-of-view (FOV) 317 x 350 mm, matrix 174 x 192, slice thickness (SL) 7 mm, 1 average, 14 segments, bandwidth (BW) 930 Hz/pix, GRAPPA x2, retrospective gating, normalized, medium smoothing filter, scan time 6–7 s/slice. There was akinetic wall motion in the territory of the left anterior descending coronary artery (LAD).

Dynamic first-pass myocardial perfusion imaging was performed in 3 short axis views (base, mid, apex) with an SR TurboFLASH pulse sequence (Fig. 2): TR 225 ms, TE 1.2 ms, FA 12°, Mag Prep Non-sel SR Perf, TI 120 ms, FOV 300 x 360 mm, matrix 120 x 192, Slice 8 mm, 1 average, 86 segments, BW 521 Hz/pix, GRAPPA x2, diastolic gating, normalized, medium smoothing filter, scan time 60 heartbeats. Single dose (0.1 mmol/kg) Multihance contrast agent was bolus

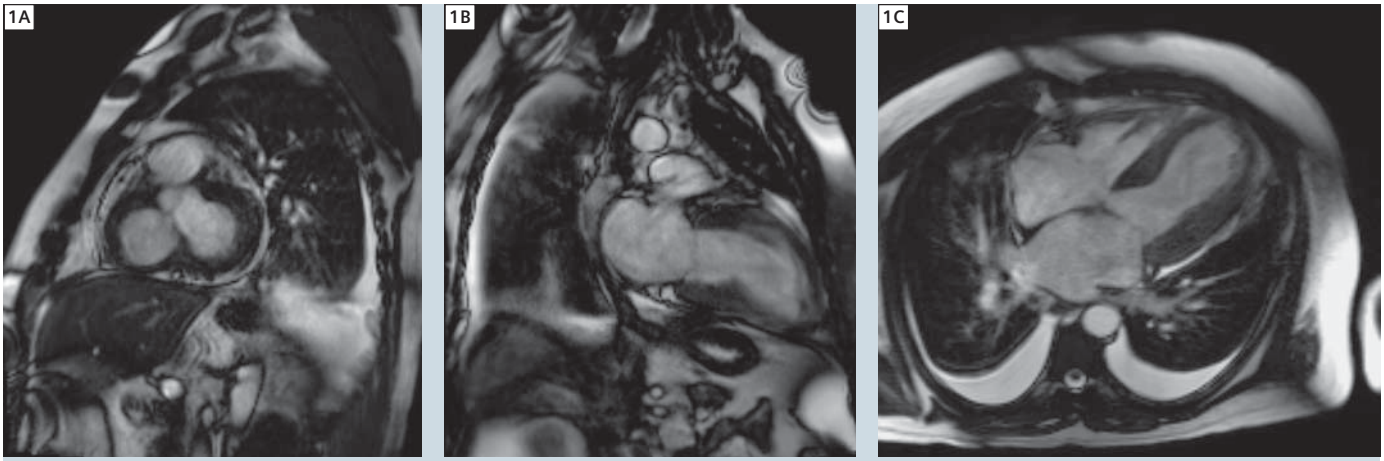

1 Segmented TrueFISP cine **(1A)**, short axis, **(1B)** 2-chamber-view, **(1C)** 4-chamber-view.

injected during first-pass scan at 3 ml/sec, flushed by 20 ml normal saline at 3 ml/sec. Patient was instructed to hold the breath for as long as possible, then breathe slow and shallow for remainder of scan. There was transmural hypo-intense signal in the LAD territory.

Post-contrast cardiac cine imaging of the myocardium was performed in multiple short axis and long axis views with a Real-time TrueFISP pulse sequence (Fig. 3): TR 117.3 ms, TE 1.0 ms, FA 59°, FOV 360 x 360 mm, matrix 121 x 160, slice 8 mm, 1 average, 51 segments, BW 1488 Hz/pix, TGRAPPA x3, normalized, medium smoothing filter, scan time 3 s/slice. There was akinetic wall motion and transmural hypo-intense signal in the LAD territory.

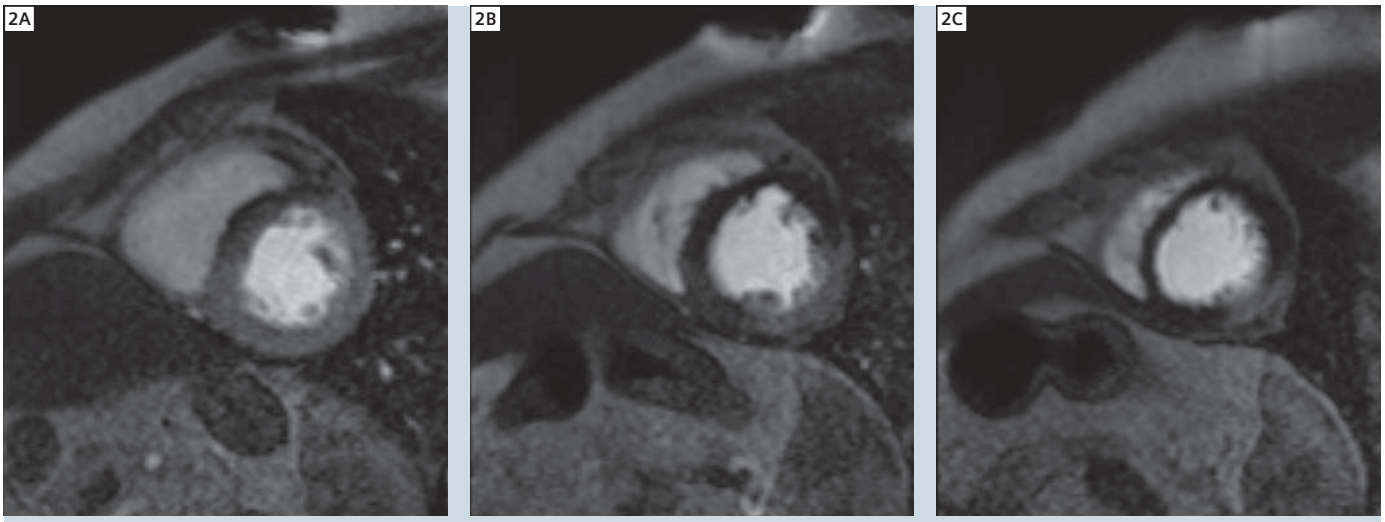

2 SR TurboFLASH first-pass perfusion: **(2A)** base, **(2B)** mid, **(2C)** apex.

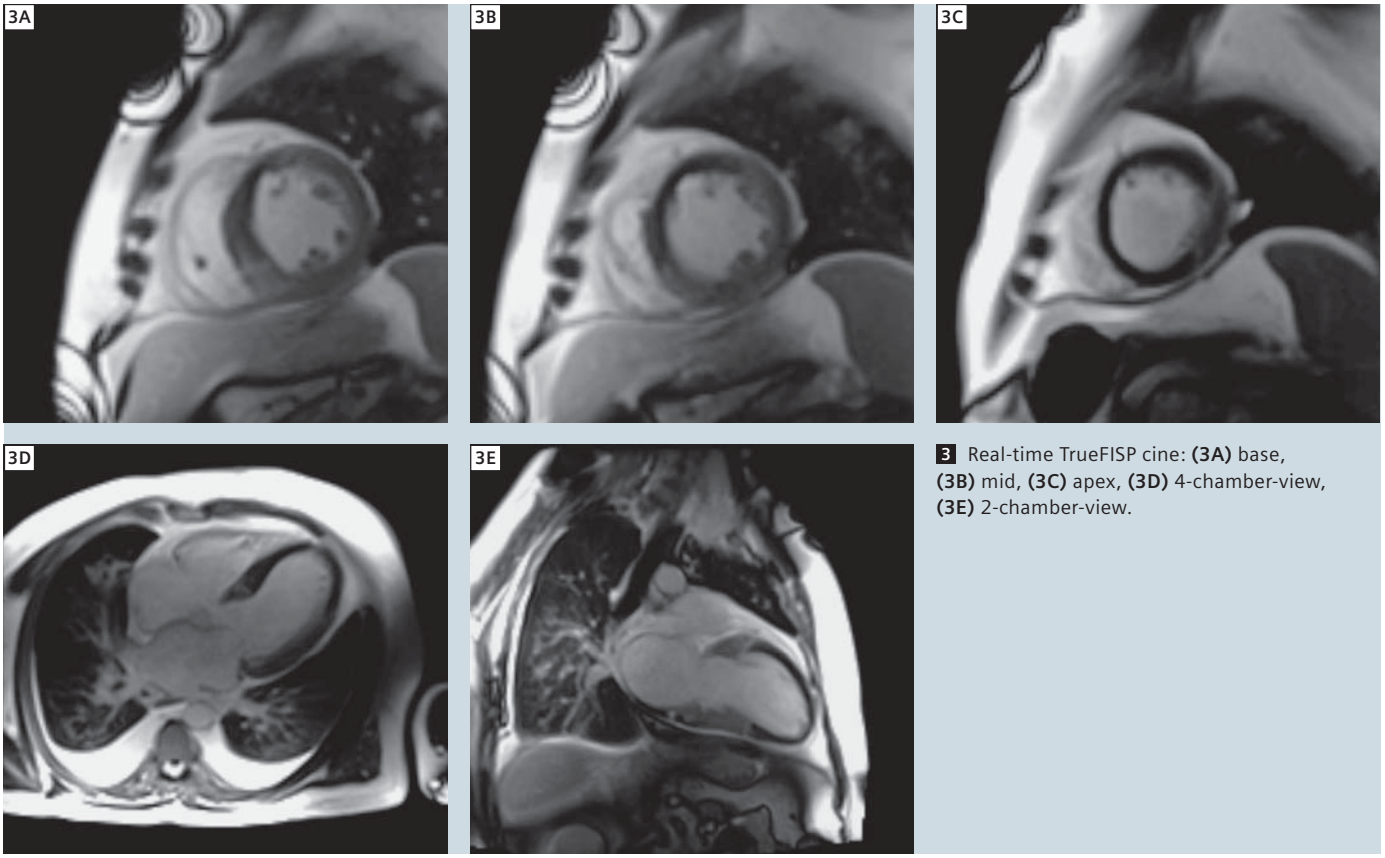

3 Real-time TrueFISP cine: **(3A)** base, **(3B)** mid, **(3C)** apex, **(3D)** 4-chamber-view, **(3E)** 2-chamber-view.

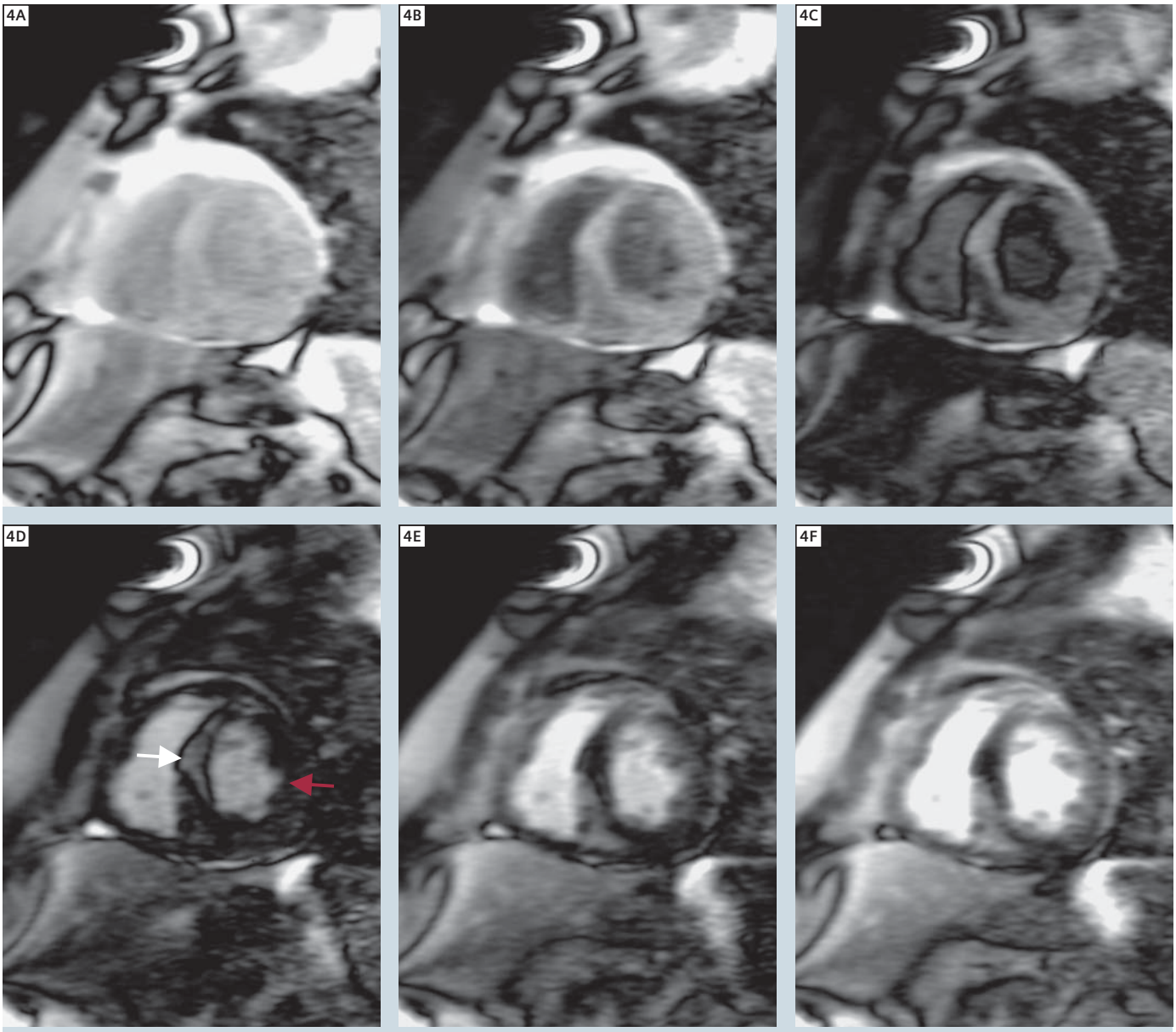

4 TI scout **(4A)** 95 ms, **(4B)** 130 ms, **(4C)** 167 ms, **(4D)** 202 ms, **(4E)** 240 ms, **(4F)** 275 ms.

TI Scout imaging was performed at a mid-ventricular level 8 minutes post-contrast using an IR TrueFISP pulse sequence (Fig. 4): TR 36.0 ms, TE 1.1 ms, FA 50°, Mag Prep TI Scout, FOV 262 x 350 mm, matrix 72 x 192, slice 7 mm, 1 average, 14 segments, BW 965 Hz/pix, normalized, medium smoothing filter, scan time 8-9 s/slice. Initially we were confused by the appearance of the septal wall. At TI 202 ms (Fig. 4D, white arrow) the antero-septal segment.demonstrates mid-grey signal intensity with surrounding dark-rim artifact which mimicks the characteristic appearance of normal myocardium at a slightly short TI time. In the next frame at TI 240 ms (Fig. 4E) the antero-septal segment.demonstrates well-nulled signal intensity with no surrounding dark-rim artifact which mimicks the typical appearance of normal myocardium at the optimal TI time. We mistakenly considered the antero-septal segment to represent normal myocardium, and we subsequently performed delayed enhancement imaging at TI 240 ms. In retrospect, the antero-septal segment actually represents abnormal myocardium whereas the lateral segment (Fig. 4D, yellow arrow) actually represents normal myocardium. As the lateral segment nulls optimally at TI 202 ms, we should have used that TI for optimal delayed enhancement imaging.

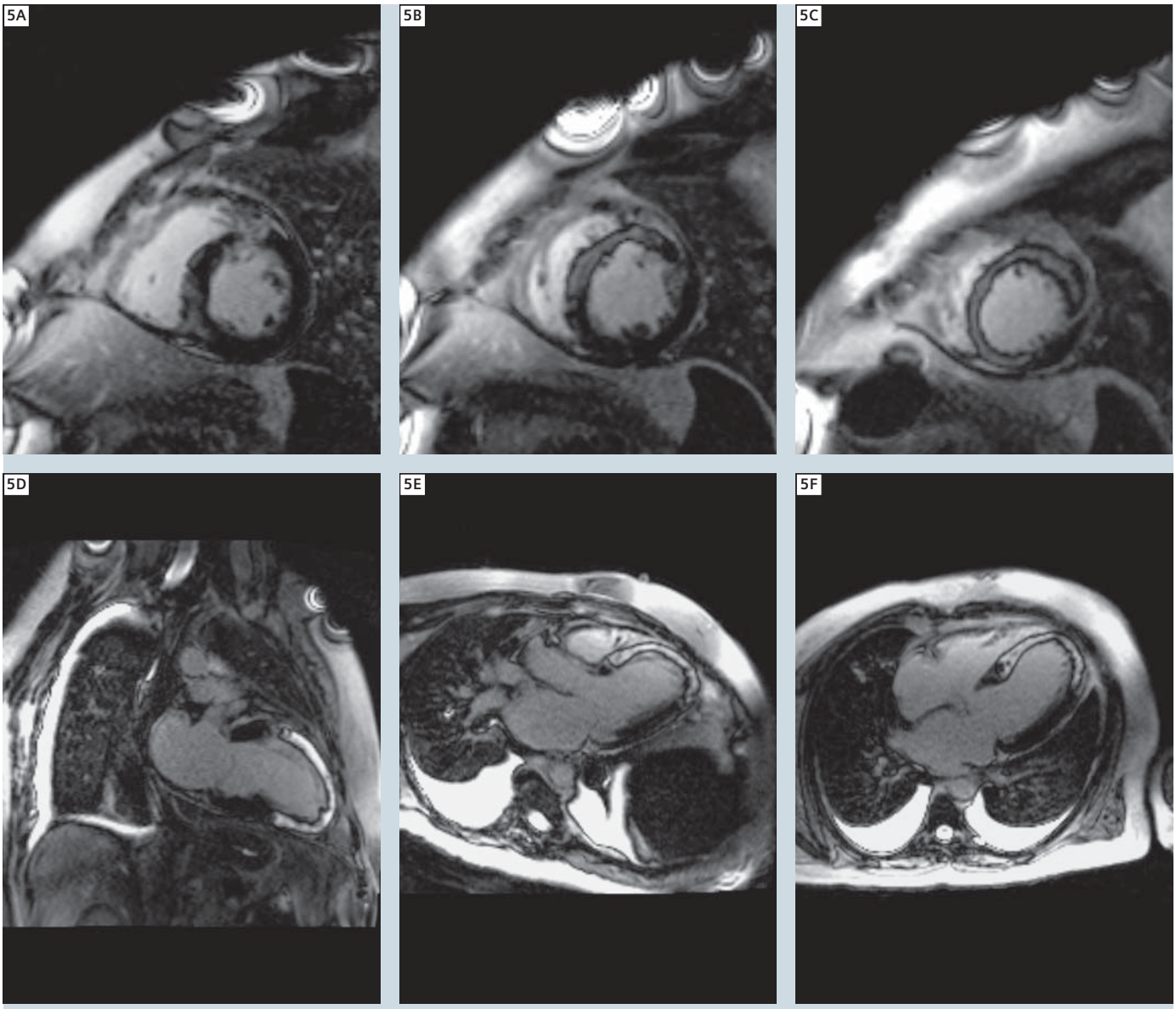

5 SS IR TrueFISP delayed enhancement TI 240 ms, MAGNITUDE images **(5A)** base, **(5B)** mid, **(5C)** apex, **(5D)** 2-chamber-view, **(5E)** 3-chamber-view, **(5F)** 4-chamber-view.

Delayed enhancement imaging was initially performed in multiple short axis and long axis views 9 minutes post-contrast using a single-shot IR TrueFISP pulse sequence (Fig. 5): TR 713 ms, TE 1.1 ms, FA 50°, Mag Prep Non-sel IR, TI 240 ms, FOV 350 x 350 mm, matrix 144 x 192, slice 8 mm, 1 average, 121 segments, BW 1184 Hz/pix, GRAPPA x2, normalized, medium smoothing filter, scan time 2 heartbeats/slice. In these MAGNITUDE images the viable myocardium appears to be well-nulled with no dark rim artifact at TI time of 240 ms, and there appears what was initially thought to be hyper-enhancement pattern in the LAD territory with an unusual dark rim artifact around the lesion. However, we subsequently determined that this bright signal in these MAGNITUDE images likely represents significant macrovascular obstruction (very long tissue T1) rather than myocardial scar (very short tissue T1).

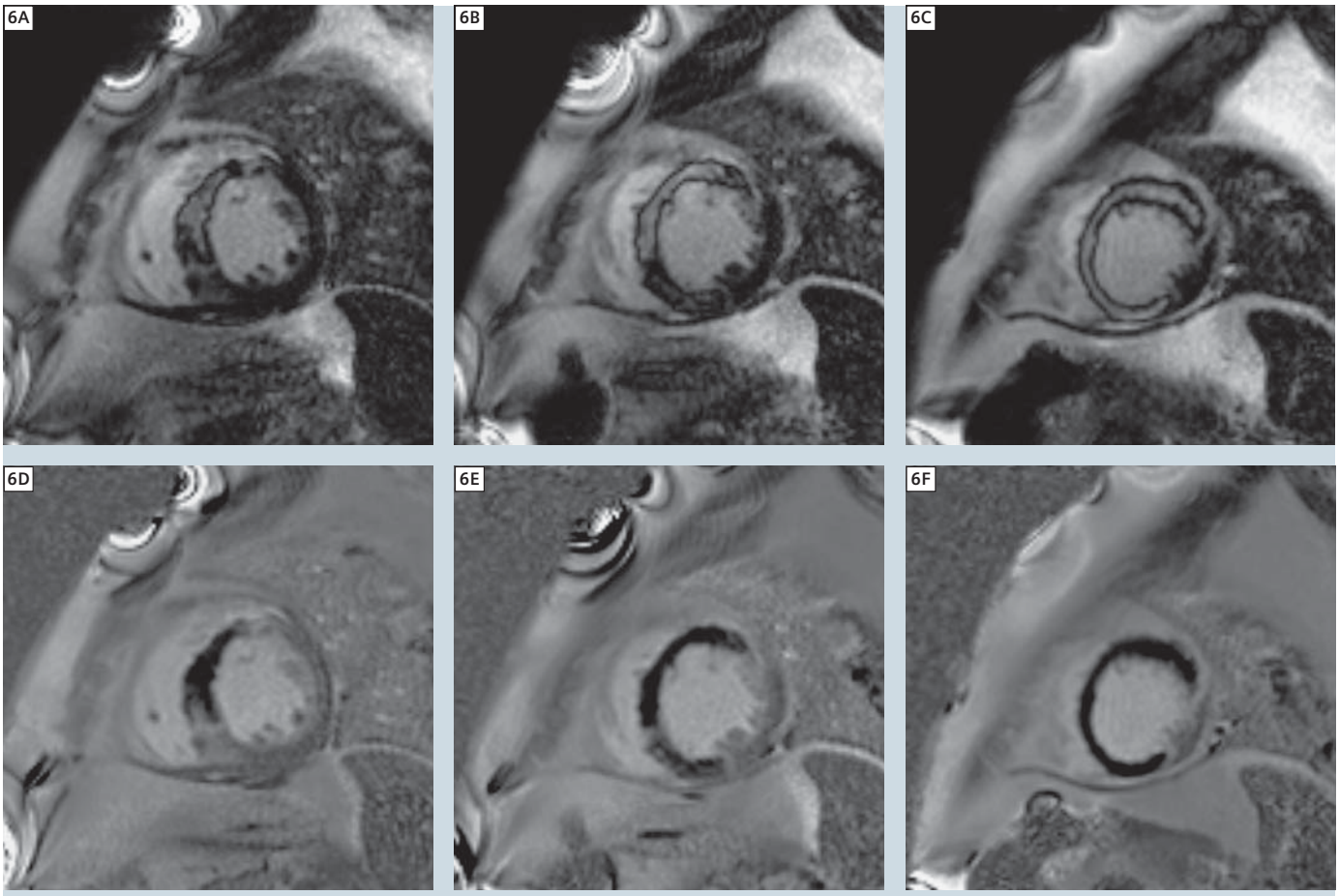

6 SS IR TrueFISP delayed enhancement TI 270 ms, MAGNITUDE images: **(6A)** base, **(6B)** mid, **(6C)** apex; PSIR images: **(6D)** base, **(6E)** mid, **(6F)** apex.

Delayed enhancement imaging was repeated in multiple short axis views 12 minutes post-contrast using a single-shot IR TrueFISP pulse sequence (Fig. 6): TR 800 ms, TE 1.1 ms, FA 40°, Mag Prep Non-sel IR, TI 270 ms, FOV 360 x 360 mm, matrix 144 x 192, slice 8 mm, 1 average, 180 segments, BW 1532 Hz/pix, GRAPPA x2, normalized, medium smoothing filter, scan time 2 heartbeats/slice. In the MAGNITUDE images there appears what was initially thought to be hyper-enhancement pattern in the LAD territory with an unusual dark rim artifact around the lesion, but otherwise good nulling in the normal myocardium. However, in the PSIR images the normal myocardium in the lateral and infero-lateral segments was intentionally windowed to a mid-grey level in order to demonstrate the much darker signal intensity in the LAD territory. The darker the signal intensity in a PSIR image, the longer its tissue T1 value. These PSIR images clearly demonstrate that the abnormal myocardium in the LAD territory has a much longer tissue T1 value than the normal myocardium elsewhere, thus suggesting no uptake of gadolinium in the LAD territory.

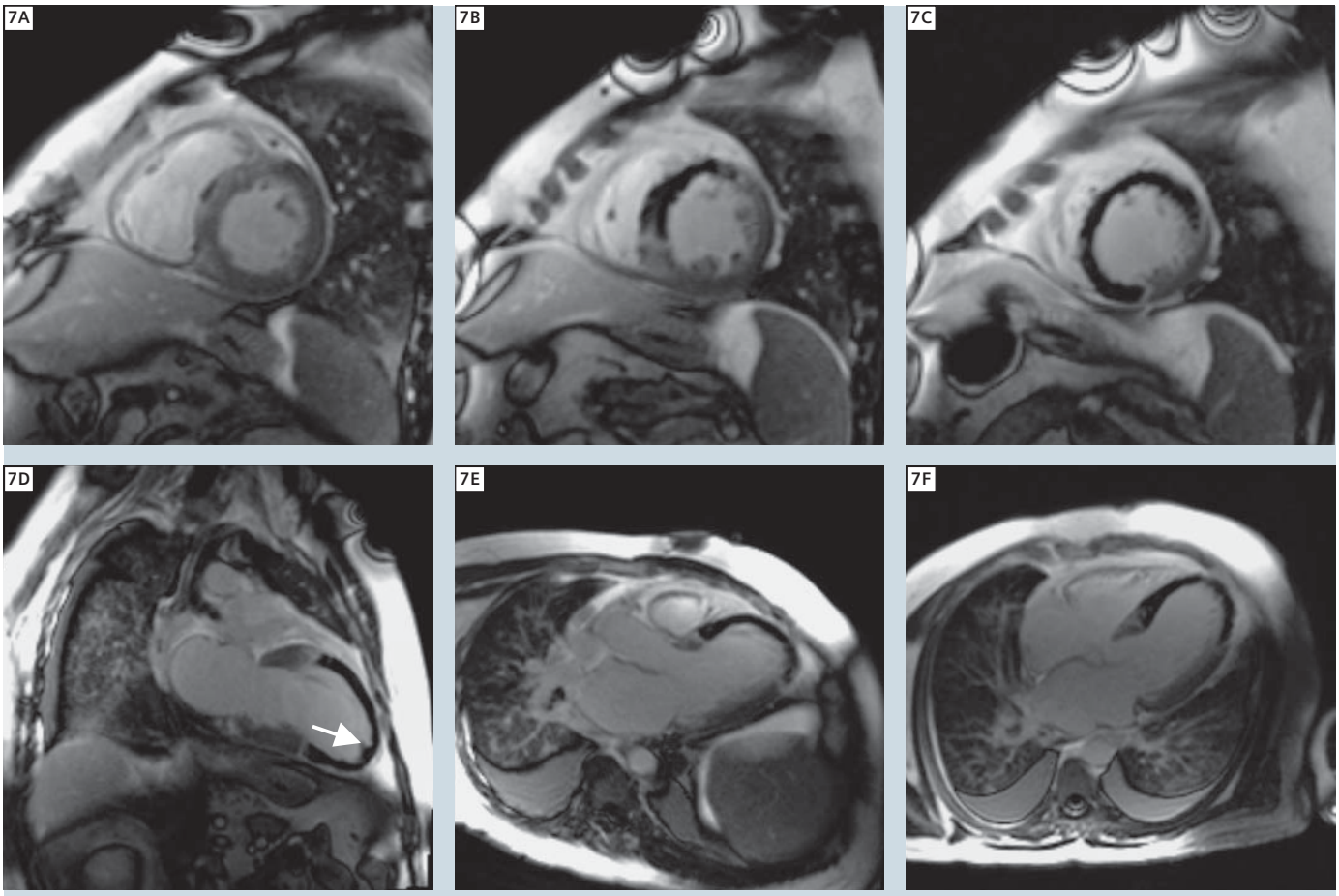

7 SS IR TrueFISP delayed enhancement TI 600 ms, MAGNITUDE images: **(7A)** base, **(7B)** mid, **(7C)** apex, **(7D)** 2-chamber-view, **(7E)** 3-chamber-view, **(7F)** 4-chamber-view.

Delayed enhancement imaging was repeated in multiple short axis and long axis views 13 minutes post-contrast using a single-shot IR TrueFISP pulse sequence (Fig. 7): TR 754 ms, TE 1.1 ms, FA 50°, Mag Prep Non-sel IR, TI 600 ms, FOV 350 x 350 mm, matrix 144 x 192, slice 8 mm, 1 average, 121 segments, BW 1184 Hz/pix, GRAPPA x2, normalized, medium smoothing filter, scan time 2 heartbeats/slice. In these MAGNITUDE images there is mid-grey signal intensity in the viable myocardium, with complete signal nulling at TI 600 ms in the LAD territory. This long TI technique is normally performed when evaluating intracavity thrombus, which appears extremely hypo-intense because it is completely avascular (white arrow). Fortunately, this technique further verified the long tissue TI of myocardium in the LAD territory likely due to macrovascular obstruction.

To corroborate the findings of non-viable myocardium in the LAD territory a Positron Emission Tomography (PET) viability study was also obtained after the CMR study (Fig. 8). Baseline resting perfusion imaging with Rubidium-82 in the Vertical Long Axis (VLA) view demonstrated absent perfusion of the entire apex, mid to apical anterior wall, and apical inferior wall. Myocardial glucose metabolism imaging with ^{18}F-fluoro-deoxyglucose (FDG) in the VLA view demonstrated absent metabolism in the same territory.

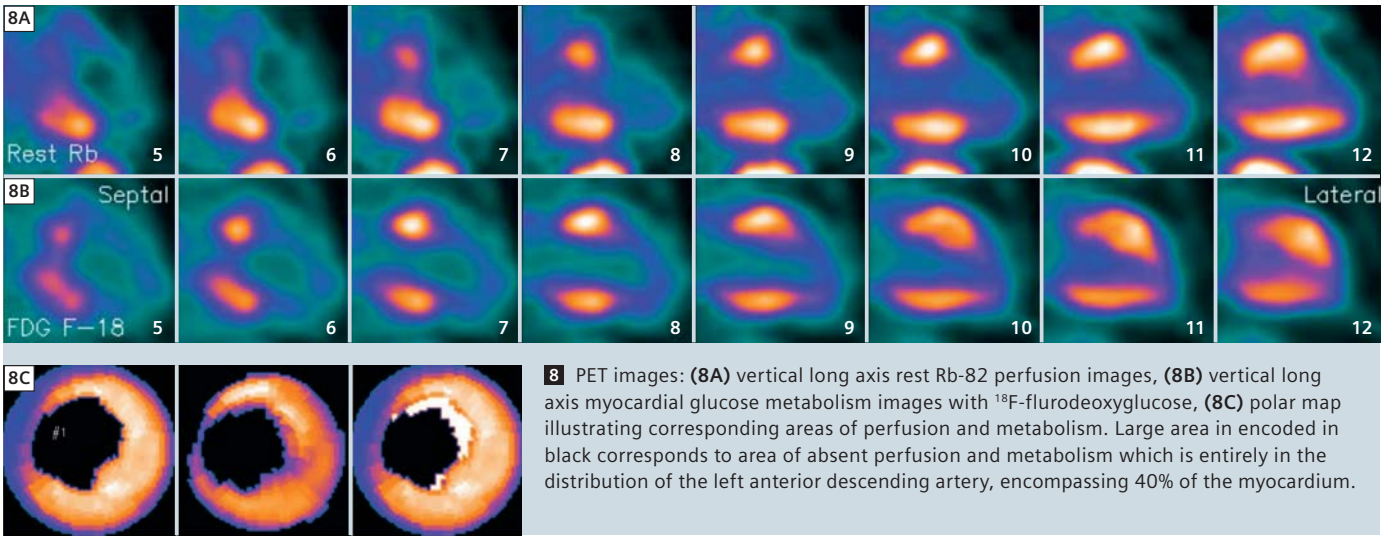

8 PET images: **(8A)** vertical long axis rest Rb-82 perfusion images, **(8B)** vertical long axis myocardial glucose metabolism images with ^{18}F-flurodeoxyglucose, **(8C)** polar map illustrating corresponding areas of perfusion and metabolism. Large area in encoded in black corresponds to area of absent perfusion and metabolism which is entirely in the distribution of the left anterior descending artery, encompassing 40% of the myocardium.

The PET study was acquired using a Siemens Biograph-40 PET/CT scanner comprised of a lutetium oxyorthosilicate (LSO) block detector ring of 162 mm FOV operating in 3D mode. Images were reconstructed dynamically (one 80-second frame, five 20-second frames, one 270-second frame) to generate time-activity curves for the left ventricular myocardium and the left ventricular cavity at a mid-ventricular level. Only frames with a greater than 2:1 average count ratio between the left ventricle and left ventricular cavity were used to generate the final static reconstruction. Diagnostic images with prompt gamma compensation (128 x 128 matrix) were reconstructed using ordered-subsets expectation maximization (OSEM) algorithm (4 iterations, 16 subsets) with a Gaussian post-filter of 7 mm.

Discussion

Initial cine imaging demonstrated akinetic wall motion in the territory of the left anterior descending artery (LAD), suggestive of either ischemia or infarct (Fig. 1). We then performed resting first-pass perfusion imaging which demonstrated an absence of contrast uptake, also suggestive of either ischemia or infarct in the LAD territory (Fig. 2). Post-contrast real time cine imaging demonstrated the same pattern of akinetic wall motion as the pre-contrast cine imaging, and also demonstrated the same absence of contrast update as the first-pass perfusion imaging (Fig. 3).

Delayed myocardial enhancement imaging was performed to evaluate for myocardial viability. The TI scout demonstrated optimal myocardial nulling at 240 ms (Fig. 4). Our initial viability images acquired at TI 240 ms demonstrated bright transmural signal in the same distribution as the dark signal appeared in the first-pass perfusion images (Fig. 5). However, the extent and morphology of the bright transmural signal was unusual, and a dark rim artifact surrounding the transmural bright signal was confounding. A bright rim artifact is typically indicative of the TI time being slightly too short for maximal nulling of viable myocardium, and thus it is not typically associated with a region of ischemia or infarct. Furthermore, in this case, the viable myocardium appears to be well-nulled with no dark rim artifact at TI time of 240 ms. We speculate that the dark rim artifact surrounding the abnormal myocardium in the LAD territory may be from fat/fluid interface cancellation, similar to that seen surrounding the pleural effusion in figures 5E, F. In retrospect, T2-weighted imaging would have been helpful to elucidate this.

To evaluate for incomplete myocardial nulling, the viability scan was repeated with a slightly longer TI of 270 ms (Fig. 6). The MAGNITUDE images again demonstrated good nulling of the normal myocardial tissue, with transmural bright signal and dark rim artifact in the LAD territory. The PSIR images demonstrated profoundly hypo-intense signal in the LAD territory with no dark rim artifact, and the viable myocardium demonstrated mid-grey signal intensity. This PSIR pattern would not be consistent with transmural scar tissue. In PSIR images, the darker the signal intensity the longer the tissue's T1 value. The observed PSIR pattern indicated that the T1 value of the abnormal tissue in the LAD territory was significantly longer than the T1 value of the remaining viable myocardium. This would be consistent with complete lack of perfusion of the entire LAD territory, likely from macrovascular obstruction.

In order to evaluate for thrombus, the viability scan was repeated with a much longer TI of 600 ms (Fig. 7). In addition to demonstrating thrombus (Fig. 7D, white arrow), the MAGNITUDE images demonstrated mid-grey signal intensity in the viable myocardium, with complete signal nulling in the LAD territory. The fact that normal myocardium nulled at TI <300 ms but the abnormal myocardium nulled at TI 600 ms confirmed that the T1 value of the abnormal myocardium was much longer than that of the normal myocardium. This could only occur if the LAD territory was completely deprived of perfusion due to extensive

macrovascular obstruction. These findings are consistent with a large myocardial infarction in the LAD territory with no evidence of viability.

Infarct scar tissue would typically be responsible for delayed hyper-enhancement signal, but no scar was identified in this patient. As predicted by the dotted lines in figure 9, MAGNITUDE images acquired at an intermediate TI 270 ms (Figs. 6A–C) demonstrated nulling of the normal viable myocardium with relatively higher signal in the obstructed myocardium. As predicted by the solid lines in figure 9, PSIR images acquired at an intermediate TI 270 ms (Figs. 6D–F) demonstrated relatively higher signal in the normal viable myocardium than the obstructed myocardium. As predicted by the solid lines in figure 9, MAGNITUDE images acquired at a long TI 600 ms (Fig. 7) demonstrated nulling of the obstructed myocardium with relatively higher signal in the normal viable myocardium.

This study illustrates findings that can be seen in macrovascular obstruction, specifically the transmural hyper-enhancement accompanied by a dark rim artifact. This finding was initially confusing because it is more commonly seen in normal myocardium which is incompletely nulled. Therefore, a PET viability study was also obtained to corroborate the CMR findings (Fig. 8). Baseline resting perfusion imaging with Rubidium-82 in the vertical long axis (VLA) view demonstrated absent perfusion of the entire apex, mid to apical anterior wall, and apical inferior wall. Myocardial glucose metabolism imaging with ^{18}F-fluorodeoxyglucose (FDG) in the VLA view demonstrated absent metabolism in the same territory. PET is considered a highly sensitive tool to detect viability. These findings are consistent with a large myocardial infarction in the LAD territory with no evidence of viability.

Clinical outcome

Non-reperfusion of the culprit vessel in STEMI portends a poor outcome. In cases where reperfusion occurs with optimal lytic therapy, death rates are reduced to 7% compared to 13% in patients treated with medical therapy alone [1–2]. In-hospital death rates can be even more substantially reduced with primary percutaneous intervention in ST-elevation myocardial infarction (STEMI) patients. The prognosis though, for any patient, varies markedly based upon each individual clinical and epidemiologic markers. In this case, the presence of diabetes mellitus, anterior wall infarction, and depressed LV function places him at substantially higher risk for cardiac morbidity and mortality. Because of this reason, an assessment of myocardial viability was deemed as a crucial element in his long term management. Unfortunately, in this case the anterior wall was non-viable and profound macrovascular obstruction was noted. Thus the patient was not referred for coronary artery bypass grafting or percutaneous intervention. Aggressive medical therapy for heart failure was initiated and the patient was referred to the heart failure service for long-term management. Because of the non-recoverability in function in the anterior wall and an LVEF of less than 35%, the patient was considered for ICD therapy. However, since early implantation of an ICD (within one month post-infarct) has not been shown to decrease mortality in high risk patients with recent myocardial infarction [3], decision was made to not implant ICD and send the patient home with a life-vest. We plan to implant an ICD at a later date if the patient's EF remains lower than 35%, which is highly likely given the large size of the non-viable lesion.

9

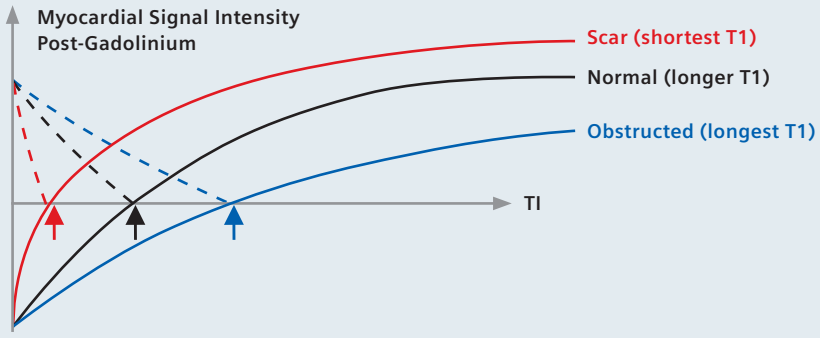

9 Signal intensity curves for three types of myocardial tissues with different T1 values. Dotted lines show the signal trajectories for MAGNITUDE images, whereas solid lines show the signal trajectories for PSIR images. **(9A)** Infarct scar tissue (red curve) would typically have the shortest T1 value and thus the shortest TI null point on MAGNITUDE images (red arrowhead). **(9B)** Normal viable myocardium (black curve) would typically have a longer T1 value and thus an intermediate TI null point on MAGNITUDE images (black arrowhead). **(9C)** Myocardial tissue which receives absolutely no perfusion due to either microvascular or macrovascular obstruction typically demonstrates the longest T1 values (blue curve) with correspondingly longer TI null points (blue arrowhead).

Acknowledgements

The authors would like to thank Dr. Edwin Wu, Northwestern University, Chicago, for his review of the manuscript and his insights regarding the appearance of macrovascular obstruction.

References

1 N Engl J Med 1993; 329:673.
2 Lancet 1999; 354:716.
3 N Engl J Med 2004; 351:2481-8.

Contact
Anurag Sahu, M.D.
Assistant Professor of Medicine
The Emory Clinic
1365 Clifton Road, NE
Atlanta, GA 30322
USA
Phone: +1 (404) 686-7878
anurag.sahu@emory.edu